J Neuropathol Exp Neurol
Vol. 77, No. 11, November 2018, pp. 1005–1016
doi: 10.1093/jnen/nly080

ORIGINAL ARTICLE

Converging Patterns of α-Synuclein Pathology in Multiple System Atrophy

Johannes Brettschneider, MD, EunRan Suh, PhD, John L. Robinson, BS, Lubin Fang, MD, Edward B. Lee, MD, PhD, David J. Irwin, MD, Murray Grossman, MD, PhD, Vivianna M. Van Deerlin, MD, PhD, Virginia M.-Y. Lee, PhD, and John Q. Trojanowski, MD, PhD

Abstract

We aimed to determine patterns of α-synuclein (α-syn) pathology in multiple system atrophy (MSA) using 70-μm-thick sections of 20 regions of the central nervous system of 37 cases with striato-nigral degeneration (SND) and 10 cases with olivo-ponto-cerebellar atrophy (OPCA). In SND cases with the shortest disease duration (phase 1), α-syn pathology was observed in striatum, lentiform nucleus, substantia nigra, brainstem white matter tracts, cerebellar subcortical white matter as well as motor cortex, midfrontal cortex, and sensory cortex. SND with increasing duration of disease (phase 2) was characterized by involvement of spinal cord and thalamus, while phase 3 was characterized by involvement of hippocampus and amygdala. Cases with the longest disease duration (phase 4) showed involvement of the visual cortex. We observed an increasing overlap of α-syn pathology with increasing duration of disease between SND and OPCA, and noted increasingly similar regional distribution patterns of α-syn pathology. The *GBA* variant, p.Thr408Met, was found to have an allele frequency of 6.94% in SND cases which was significantly higher compared with normal (0%) and other neurodegenerative disease pathologies (0.74%), suggesting that it is associated with MSA. Our findings indicate that SND and OPCA show distinct early foci of α-syn aggregations, but increasingly converge with longer disease duration to show overlapping patterns of α-syn pathology.

Key Words: Multiple system atrophy, Pathology, Synuclein.

INTRODUCTION

Multiple system atrophy (MSA) is a progressive adult-onset neurodegenerative disease of yet unknown etiology (1) that includes 2 major pathological subtypes: Olivo-ponto-cerebellar atrophy (OPCA), clinically defined by cerebellar ataxia, and striato-nigral degeneration (SND), presenting as a Parkinsonian syndrome poorly responsive to dopaminergic therapy (2–4). While SND is more frequent in Western countries, Japan shows a predominance of OPCA (5, 6). The clinical features of both subtypes to a variable extent include autonomic failure which can predate motor symptoms (1, 7). While MSA is generally believed to be sporadic disease, emerging evidence has suggested rare genetic variants that increase susceptibility to the disease (8–11).

The neuropathological hallmarks of MSA are α-synuclein (α-syn)-positive (oligodendro-) glial cytoplasmic inclusions (GCI) and, to a lesser extent, neuronal inclusions (NI) in the central nervous system (CNS) (2, 12, 13). α-Syn is a ∼17-kDa protein that is predominantly expressed in neurons where it localizes to the synaptic terminal and presumably plays a role in vesicle transport and exocytosis (14–16). When misfolding occurs, the random coil of its NAC region forms β-sheets, leading to protofibril and fibril formation that accumulate into aggregates. Similar α-syn aggregates also characterize pathology of Parkinson disease (PD) and dementia with Lewy bodies (DLB), albeit in a predominantly neuronal localization (17).

Progressive spreading of nonprion protein aggregates is a unifying pathological principle of clinically diverse neurodegenerative diseases including synucleinopathies (18–20). However, given the mainly oligodendroglial localization of α-syn aggregates in MSA, which sets it apart from other synucleinopathies, it is currently unclear if this concept of protein propagation can be extended to MSA.

We aimed to determine early foci and spreading patterns of α-syn pathology in SND by implementing a methodological approach that allows a highly sensitive analysis of protein aggregation pathology and its anatomical localization in neurodegenerative diseases (21), an approach which has been previously applied to analyze sequential spreading of α-syn pathology in PD (22).

From the Center for Neurodegenerative Disease Research (CNDR), University of Pennsylvania School of Medicine, Philadelphia, Pennsylvania (JB, JLR, EBL, DJI, MG, VM-YL, JQT); Clinical Neuroanatomy Section, Department of Neurology, Center for Biomedical Research, University of Ulm, Ulm, Germany (LF); and Department of Pathology and Laboratory Medicine, University of Pennsylvania School of Medicine, Philadelphia, Pennsylvania (ES, EBL, DJI, MG, VMVD, VM-YL, JQT).

Send correspondence to: John Q. Trojanowski, MD, PhD, CNDR, University of Pennsylvania School of Medicine, 3rd Floor Maloney Building, 3600 Spruce Street, Philadelphia, PA 19104; E-mail: trojanow@upenn.edu

This study was supported by a grant from The MSA Coalition/Cure PSP to Johannes Brettschneider and an NINDS funded Morris K. Udall Parkinson's Disease Research Center of Excellence (P50 NS053488). VM-YL is the John H. Ware, 3rd, Professor of Alzheimer's Disease Research. John Q. Trojanowski is the William Maul Measey-Truman G. Schnabel, Jr. Professor of Geriatric Medicine and Gerontology.

The authors have no duality or conflicts of interest to declare.

Supplementary Data can be found at academic.oup.com/jnen.

MATERIALS AND METHODS

Autopsy Cohort

We included 47 patients with a neuropathological diagnosis of definite MSA (2, 23, 24) (16 females, 31 males; mean age at onset ± SD: 58 ± 9.8 years, range 39–82 years, mean disease duration ± SD: 7.2 ± 3.5 years, range 2–17 years) followed to autopsy in the Center for Neurodegenerative Disease Research (CNDR) at the University of Pennsylvania between 1989 and 2013.

Our cohort included 37 cases with SND (15 females, 22 males; mean age at onset ± SD: 58 ± 10.5 years, range 39–82 years, mean disease duration ± SD: 7.5 ± 3.6 years, range 2–17 years) (24) and 10 cases with OPCA (1 female, 9 males; mean age at onset ± SD: 58 ± 7.7 years, range 51–74 years, mean disease duration ± SD: 6.1 ± 3.3 years, range 3.5–14 years), which were previously described in detail by our group (25).

Written informed consent was obtained from all patients or from their next of kin. Detailed clinical characteristics (gender, age at onset, age at death, clinical symptoms of onset, disease duration) were ascertained from an integrated autopsy database, as described previously (26, 27) and by retrospective chart review of clinical visits within the University of Pennsylvania Health System (Table). Throughout this text, "disease duration" describes the duration of clinical symptoms in the individual patient.

Tissue Preparation, Staining, and Immunohistochemistry

Pathology was examined in the following regions of the CNS (Supplementary Data Fig. S1): Midfrontal cortex, orbital frontal cortex, motor cortex, sensory cortex, superior or middle temporal gyrus (SMT), angular cortex, visual cortex, anterior cingulate gyrus, amygdala, hippocampus, striatum, lentiform nucleus, thalamus, midbrain, upper pons, lower pons, medulla oblongata, cerebellum, and cervical spinal cord (CSC). Additional blocks of spinal cord sections (thoracic SC, lumbar SC, and sacral SC) were available for 5 cases.

After fixation, tissue samples were embedded in paraffin using standardized cassettes, sectioned at 6–7 µm, and stained with hematoxylin and eosin and for immunohistochemistry as previously described elsewhere (28, 29). Briefly, immunohistochemistry was performed with antibodies to α-syn (monoclonal antibody Syn303; 1:4000, generated in CNDR) (30), hyperphosphorylated tau (monoclonal antibody PHF1; 1:1000, gift from Dr. Peter Davies), pTDP-43 (rat antibody p409/410, 1:1000, gift from Dr. Manuela Neumann) (31), and amyloid-β (monoclonal antibody NAB228; 1:15 000; generated in CNDR) (32). Neurofibrillary tangle stages and CERAD neuritic plaque scores are shown in Table.

To study each of the CNS regions in all 47 cases in greater neuroanatomical detail, additional sets of 70-µm sections were prepared as described previously (21) from the same paraffin blocks as used above. This thick section technique is performed on free-floating sections and permits accurate anatomical localization of pathological changes in synucleinopathies, tauopathies, and pTDP-43 proteinopathies (21). The sections were stained for analysis of α-syn pathology as well as for topographical overview and neuronal loss using a pigment-Nissl stain for lipofuscin pigment (aldehyde fuchsin) and basophilic Nissl material (Darrow red) in combination with the α-syn antibody described above.

Severity of α-syn pathology was assessed based on analysis of thick sections according to a semiquantitative rating scale (0, absent or not detectable; ≤2 aggregates per region; +, mild; ++, moderate; and 3, severe/numerous +++) (22). Severity of neuronal α-syn pathology was throughout adjusted for neuronal loss. Neuronal loss was rated semiquantitatively as follows: 0 = absent; + = mild; ++ = moderate; and +++ = severe.

Genetic Testing

Genomic DNA was extracted from fresh frozen brain tissues using QIAamp DNA mini kit (Qiagen, Germantown, MD) following manufacturer recommendations. The coding and flanking intronic regions of 45 neurodegenerative disease-associated genes, including *COQ2*, *SNCA*, and *glucocerebrosidase (GBA)*, were sequenced using a targeted next generation sequencing (NGS) panel, MiND-Seq (Multi Neurodegenerative Disease Sequencing panel) (25, 26). Libraries of the target regions prepared used the Haloplex enrichment kit (Agilent Technologies, Santa Clara, CA) according to the manufacturer's protocol were sequenced on a HiSeq sequencer (Illumina, San Diego, CA). Alignment of sequence reads and variant calling from NGS were assessed by SureCall software (Agilent, Santa Clara, CA). Exons with poor depth of coverage by next generation sequencing (COQ2 exons 1 and 7) were individually Sanger sequenced (primers and conditions available on request). Genotyping of *GBA* c.1223C>T, p.Thr408Met (rs75548401) was performed using a TaqMan allelic discrimination assay (Applied Biosystems, Waltham, MA).

Statistical Analysis

Data analysis was performed using SPSS (Version 17.0 SPSS Inc., Chicago, IL). The average (and range) of data on patient characteristics was estimated by calculating the median (and 25–75th percentiles). Differences between 2 clinical subgroups were compared using Wilcoxon Mann-Whitney test. To compare raw data of multiple subgroups, Kruskal-Wallis analysis of variance on ranks was applied and in case of significance, by Dunn's Method. Trend analysis was conducted using the Mantel-Haenszel Chi-square test. All correlations were studied using Spearman's rank order correlation coefficient. Bonferroni-correction for multiple testing was applied when contrasts were not driven by a specific hypothesis. The Fisher exact test was performed to analyze the genetics data. For all other tests, p values <0.05 were considered significant. All statistical tests were 2-sided.

RESULTS

Main Types of α-Syn Pathology in MSA

The most abundant α-syn pathology in both SND and OPCA consisted of GCI in white and—to a lesser extent—grey matter oligodendroglia (Fig. 1A). In addition, we

TABLE. Demographic Data, Clinical Symptoms, and Tau and Abeta Pathology in SND and OPCA Cases

No.	Type	Age at Onset [Years]	Disease Duration [Months]	Initial Clinical Syndrom	Park	Aut	Cer	Pyr	Sen	Cog	NFT	Abeta
1	SND	70	48	UMN	No	Yes	No	Yes	No	No	2	0
2	SND	70	48	Parkinsonism	Yes	Yes				Yes	1	0
3	SND	63	48	Autonomous	Yes	Yes	No	No	No		1	1
4	SND	49	24	Autonomous	Yes	Yes	No	No	Yes	No	0	1
5	SND	64	36	Parkinsonism	Yes	Yes	Yes	No	No	No	0	0
6	SND	82	48	Parkinsonism	Yes	Yes					1	2
7	SND	61	72	Parkinsonism	Yes	Yes	No	Yes	Yes	No	1	2
8	SND	39	48	Parkinsonism	Yes	Yes					0	0
9	SND	74	60	Parkinsonism	Yes	Yes	No	No	No	No	2	2
10	SND	47	72	Parkinsonism	Yes	Yes					0	0
11	SND	54	48	Parkinsonism	Yes	Yes	No	No	No	No	1	1
12	SND				Yes	Yes				No	0	1
13	SND	71	60	Parkinsonism	Yes	Yes	No	No	No	Yes	2	0
14	SND	56	60	Autonomous	Yes	Yes	Yes	No	No	No	1	0
15	SND	73	48	Parkinsonism	Yes	Yes				No	1	0
16	SND	50	84	Parkinsonism	Yes	Yes		Yes		No	2	0
17	SND	56	84	Parkinsonism	Yes	Yes	No	No	No	Yes	0	0
18	SND	62	84	Parkinsonism	Yes	Yes	No	No	No	No	2	2
19	SND	56	96	Parkinsonism	Yes	Yes	No	No	No	No	1	0
20	SND	59	72	Parkinsonism	Yes	Yes	No	Yes	No	No	0	0
21	SND				Yes	Yes				Yes	2	2
22	SND	61	96	Parkinsonism	Yes	Yes	Yes	No	Yes	No	1	0
23	SND	48	84		Yes	Yes	No	No	No	Yes	0	1
24	SND	46	90	Parkinsonism	Yes	Yes	No	No	No	No	0	1
25	SND	51	108	Parkinsonism	Yes	Yes	No	Yes	No	No	0	0
26	SND	57	180	Parkinsonism	Yes	Yes		Yes			1	3
27	SND	63	120	Parkinsonism	Yes	Yes				Yes	1	1
28	SND	56	204	Parkinsonism	Yes	Yes	No	Yes	No	No	1	0
29	SND	45	108	Parkinsonism	Yes	Yes				No	0	0
30	SND	47	120	Autonomous	Yes	Yes	No	No	No	No	0	1
31	SND	62	108	Parkinsonism	Yes	Yes	No	No	Yes	No	1	0
32	SND	67	108	Parkinsonism	Yes	Yes	No	No	No	No	0	1
33	SND				Yes	Yes					1	1
34	SND	47	144		Yes						0	0
35	SND	60	144	Parkinsonism	Yes	Yes	No			No	0	0
36	SND			Parkinsonism	Yes						0	0
37	SND				Yes					Yes	0	0
38	OPCA	55	45	Autonomous	No	Yes	Yes	No	No	No	0	0
39	OPCA	53	48	Cerebellar	No	Yes	Yes	No	No	No	1	2
40	OPCA	62	42	Cerebellar	Yes	Yes	Yes				1	0
41	OPCA	69	72	Cerebellar	No	Yes	Yes	Yes	No	No	0	0
42	OPCA	53	48	Cerebellar	No	Yes	Yes				0	0
43	OPCA	74	66	Cerebellar	Yes	Yes	Yes	Yes	Yes	No	0	0
44	OPCA	51	49	Cerebellar	No	Yes	Yes	No	Yes	No	2	0
45	OPCA	53	168	Cerebellar	Yes	Yes	Yes	Yes	No	No	0	0
46	OPCA	54	108	Cerebellar		Yes	Yes				1	0
47	OPCA	55	84	Cerebellar		Yes	Yes				0	2

Abbreviations: Aut = autonomous dysfunction, Cer = cerebellar syndrome, Cog = cognitive deficits, NFT = neurofibrillary tangles, No. = case number, OPCA = olivo-ponto-cerebellar atrophy, Park = Parkinson syndrome, Pyr = clinical signs of pyramidal involvement, Sen = clinical signs of sensory involvement, SND = striatonigral degeneration, Type = neuropathological subtype of MSA, UMN = upper motor neuron syndrome.

observed neuritic inclusions (NRI), which presented as long axonal or dendritic α-syn aggregates (Fig. 1D). NI were mostly cytoplasmic but occasionally nuclear, as previously described (25) and were neither as severe nor as widespread as GCI. NI only gradually developed with increasing overall burden of pathology. Neuronal loss was frequently observed to

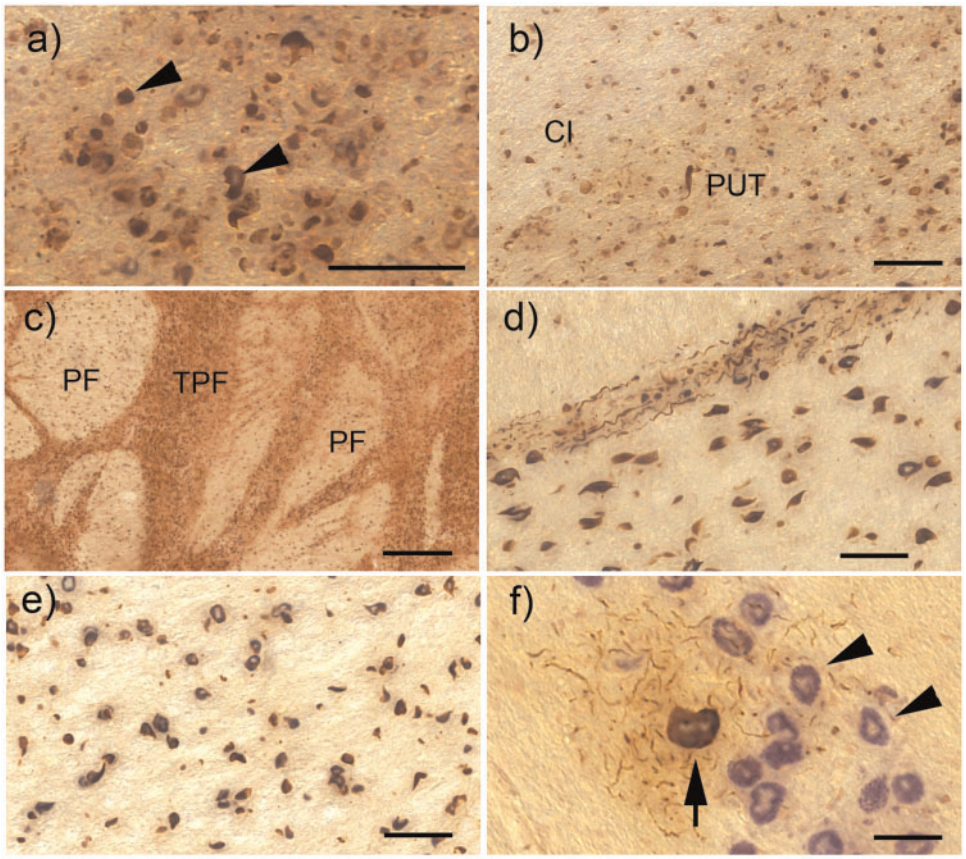

FIGURE 1. α-Synuclein pathology in the basal ganglia, pons, and medulla of cases with SND. All images here and in the subsequent figures showing α-syn immunohistochemistry are combined with pigment-Nissl stain for lipofuscin pigment (aldehyde fuchsin) and basophilic Nissl material (Darrow red). **(A)** Glial cytoplasmic α-syn inclusions (GCI) in oligodendroglia of the internal capsule (some of the GCI are indicated by arrowheads). **(B)** Overview of GCI pathology in the internal capsule (CI) and putamen (PUT). **(C)** Severe GCI pathology in the pons within transverse pontine fibers (TPF) and fibers of the corticospinal tract (PF). **(D)** GCI in the TPF and PF also showing multiple neuritic inclusions (NRI) within the TPF. **(E)** GCI in the PF of the medulla. **(F)** Neuronal cytoplasmic α-syn inclusion (NI) in the inferior olive of the medulla (arrow), surrounded by multiple NRI and the unaffected inferior olive neurons (arrowheads). All scale bars = 50 μm; scale bar in **(C)** = 500 μm.

affect groups of neurons that did not (or only to a very mild extent) show NI.

Phases of α-Syn Pathology in SND

Based on the different types of α-syn inclusions as described above, we proceeded to analyze phases of α-syn pathology in SND cases with increasing disease duration and pathology burden (Table), aiming to delineate early foci of α-syn aggregation.

Phase 1: Involvement of Basal Ganglia, Brainstem, and Cortex

In SND cases with the shortest disease duration (n = 3, mean disease duration of 48 months, Fig. 2A), most severe α-syn pathology was observed in the striatum and lentiform nucleus. Blocks of the striatum showed severe GCI in the white matter of the internal capsule (Fig. 1B), as well as in putaminal grey matter, while involvement of the caudate nucleus was less severe. Within blocks of the lentiform nucleus, GCI were observed in both putamen and pallidum, with the putamen more severely affected.

In the SN of the midbrain, GCI and NRI were observed among neurons of both pars compacta and pars reticulata. Furthermore, GCI were detectable in the crus cerebri, with most severe aggregates detectable in the middle parts of the crus cerebri, and did also mildly involve the medial lemniscus.

In the pons, the most severe pathology affected the transverse pontine fibers and pyramidal fibers as well as the middle cerebellar peduncle (Figs. 1C, D, 2A). In the medulla, pathology involved pyramidal white matter (Fig. 1E) as well as the medial lemniscus and the medullary internal white matter (area posterior of the inferior olive, lateral to the medial lemniscus, including the olivo-cerebellar fibers, internal arcuate fibers, as well as spinocerebellar tract fibers, Supplementary Data Fig. S2). NI were also observed in the inferior olive (Fig. 1F), and became more severe in cases with a longer disease duration.

Cerebellar pathology was already detectable in SND phase 1 cases. It was most severe in the subcortical white

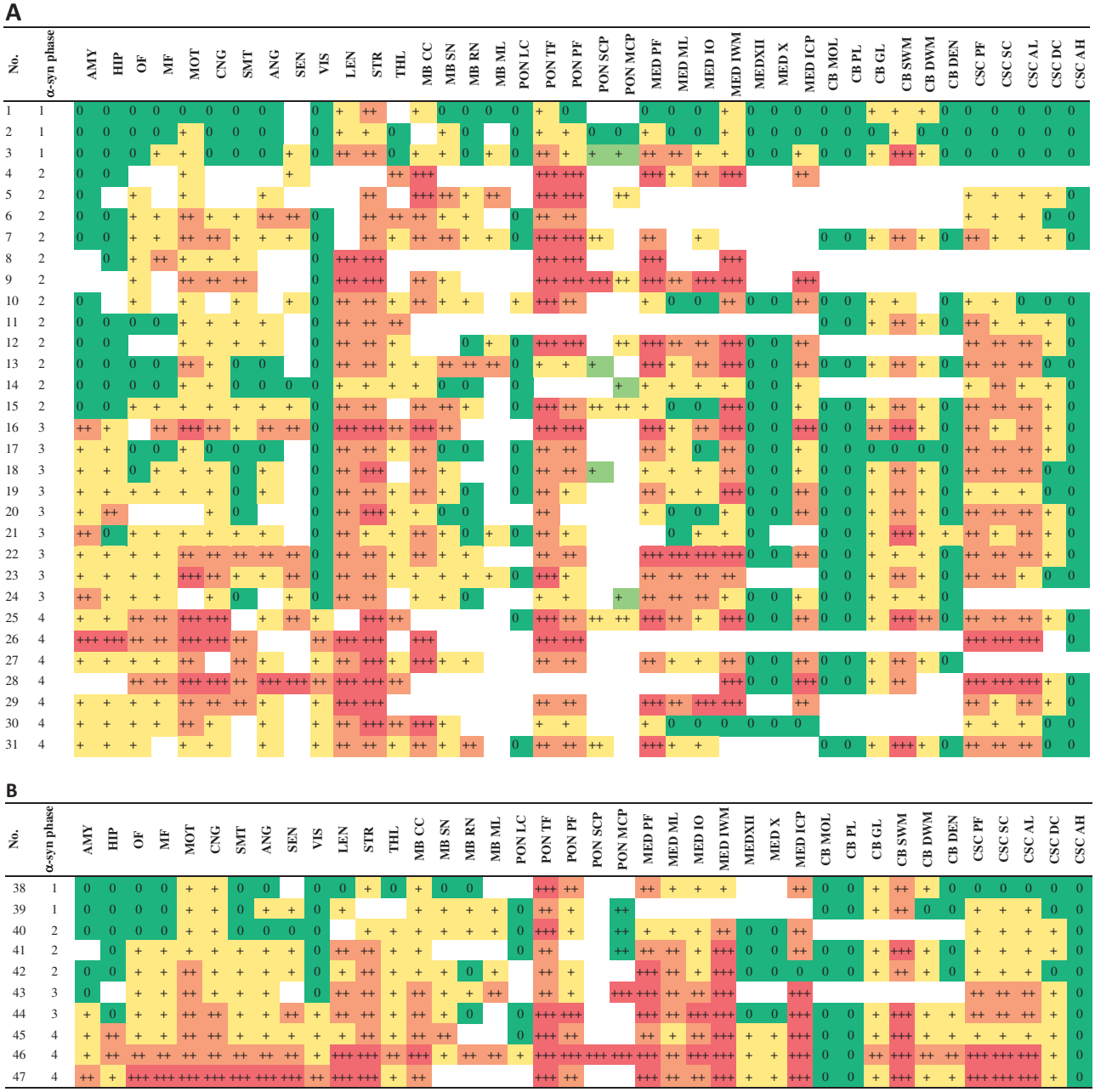

FIGURE 2. (**A**) Severity of α-syn pathology in striato-nigral degeneration (SND). Color-coding reflects severity of pathology from green color = no pathology to red color (= severe pathology). **(B)** Severity of α-syn pathology in olivo-ponto-cerebellar atrophy (OPCA). *Abbreviations:* AMY = amygdala, ANG = angular cortex, CB DEN = cerebellum dentate nucleus, CB DWM = cerebellum deep white matter, CB GL = cerebellum granular layer, CB MOL = cerebellum molecular layer, CB PL = cerebellum Purkinje cell layer, CB SWM = cerebellum subcortical white matter, CNG = anterior cingulate gyrus, CSC AH = cervical spinal cord anterior horn, CSC AL = cervical spinal cord anterolateral fibers, CSC DC = cervical spinal cord dorsal column, CSC PF = cervical spinal cord pyramidal fibers, CSC SC = cervical spinal cord spinocerebellar fibers, HIP = hippocampus, LEN = lentiform nucleus, MB CC = midbrain crus cerebri, MB ML = midbrain medial lemniscus, MB RN = midbrain red nucleus, MB SN = midbrain substantia nigra, MED ICP = medulla inferior cerebellar peduncle, MED IO = medulla inferior olive, MED IWM = medulla internal white matter, MED ML = medulla medial lemniscus, MED PF = medulla pyramidal fibers, MED X = medulla dorsal motor nucleus of the vagus, MED XII = medulla hypoglossal nucleus, MF = midfrontal cortex, MOT = motor cortex, OF = orbital frontal cortex, PON LC = pons locus coeruleus, PON MCP = pons middle cerebellar peduncle, PON PF = pons pyramidal fibers, PON SCP = pons superior cerebellar peduncle, PON TF = transverse pontine fibers, SEN = sensory cortex, SMT = superior and middle temporal gyrus, VIS = visual cortex, STR = striatum, THL = thalamus.

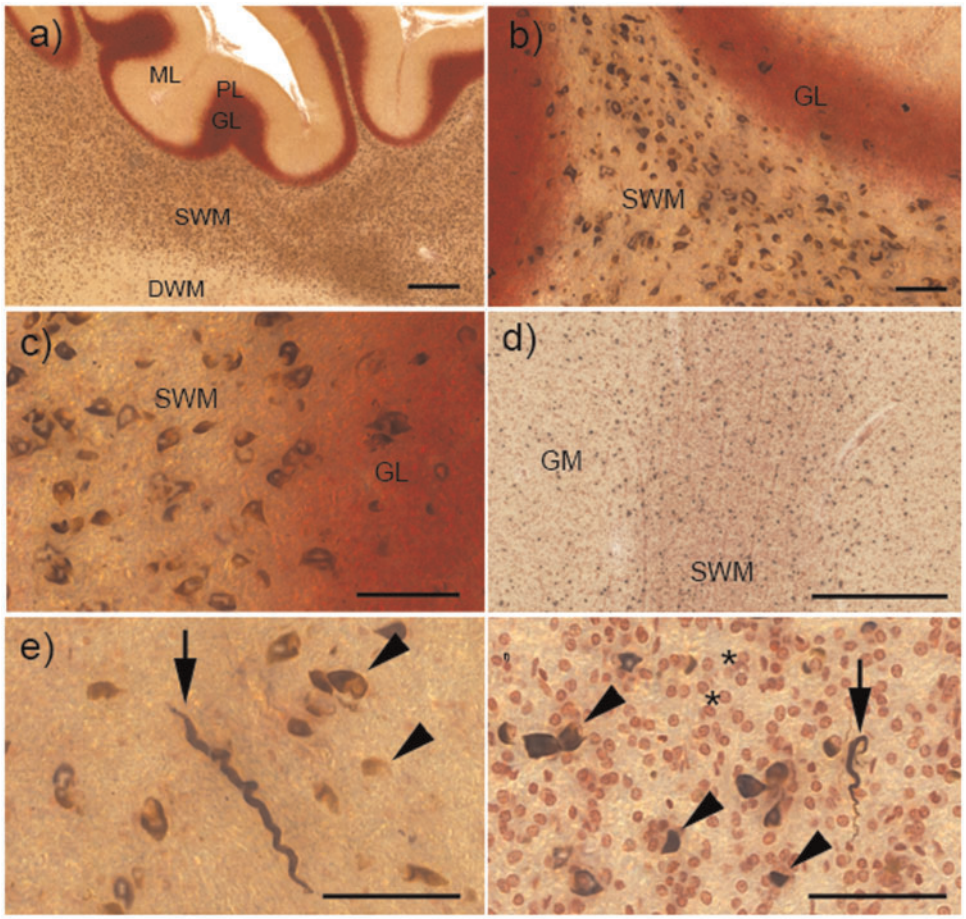

FIGURE 3. α-Synuclein (α-syn) pathology in the cerebellum and cortex of cases with striatonigral degeneration (SND). **(A)** Overview of glial cytoplasmic inclusions (GCI) in different layers of the cerebellar cortex. While severe GCI pathology is present in the subcortical white matter (SWM), deep white matter (DWM) and granular layer (GL) are much less involved, and molecular layer (ML) and Purkinje cell layer (PL) show no GCI. **(B, C)** Higher-resolution images show severe GCI in the SWM and milder pathology in the GL. **(D)** GCI pathology in the grey matter (GM) and SWM of the orbital frontal cortex. **(E)** Neuritic inclusions (NRI, arrow) and GCI (arrowheads) in the cortical GM. **(F)** Neuritic inclusions (NRI, arrow) and GCI (arrowheads) in the SWM, small reddish oligodendroglia without GCI are shown by asterisks. All scale bars = 50 μm; scale bars in **(A)** and **(D)** = 500 μm.

matter, while the granular layer and deep white matter were only mildly involved (Fig. 3A–C). In contrast, the molecular layer and Purkinje cell layer as well as the dentate nucleus were spared (Fig. 2A).

Phase 1 cases of SND also already showed cortical α-syn aggregates (Fig. 2A). Cortical pathology was generally mild and, in this phase, they were limited to motor cortex, midfrontal cortex, and sensory cortex. Within the cortex, α-syn aggregates were mainly found in subcortical white matter, but also mildly involved cortical grey matter (Figs. 2A, 3D–F). Amygdala and hippocampus were uninvolved in these cases, as were thalamus and CSC.

Phase 2: Involvement of CSC and Thalamus

SND cases with increasing duration of disease (n = 12, mean duration of disease 52.3 months ± 14.5 months) were characterized by an additional involvement of spinal cord and thalamus. Within the spinal cord, GCI were observed in the pyramidal tract, as well as in the spino-cerebellar and spino-thalamic tracts (Fig. 2A). In contrast, involvement of the dorsal column was generally much less severe (Fig. 3A–C). GCI could be observed among the neurons of the anterior horn, but no NI and NRI were detected in these cells. In the midbrain, α-syn pathology became more severe and could also involve the red nucleus (Fig. 2A). Cortical involvement became more widespread in these cases, and spread to involve the orbital gyri, anterior cingulate gyrus, SMT, and angular cortex (Fig. 2A). In contrast, the visual cortex remained free of pathology in all phase 2 cases.

Phase 3: Involvement of Hippocampus and Amygdala

Cases with further increasing duration of disease (n = 9, mean duration of disease 86.3 months ± 7.8 months) were characterized by involvement of hippocampus and amygdala (Fig. 2A). Within the hippocampus, α-syn inclusions were

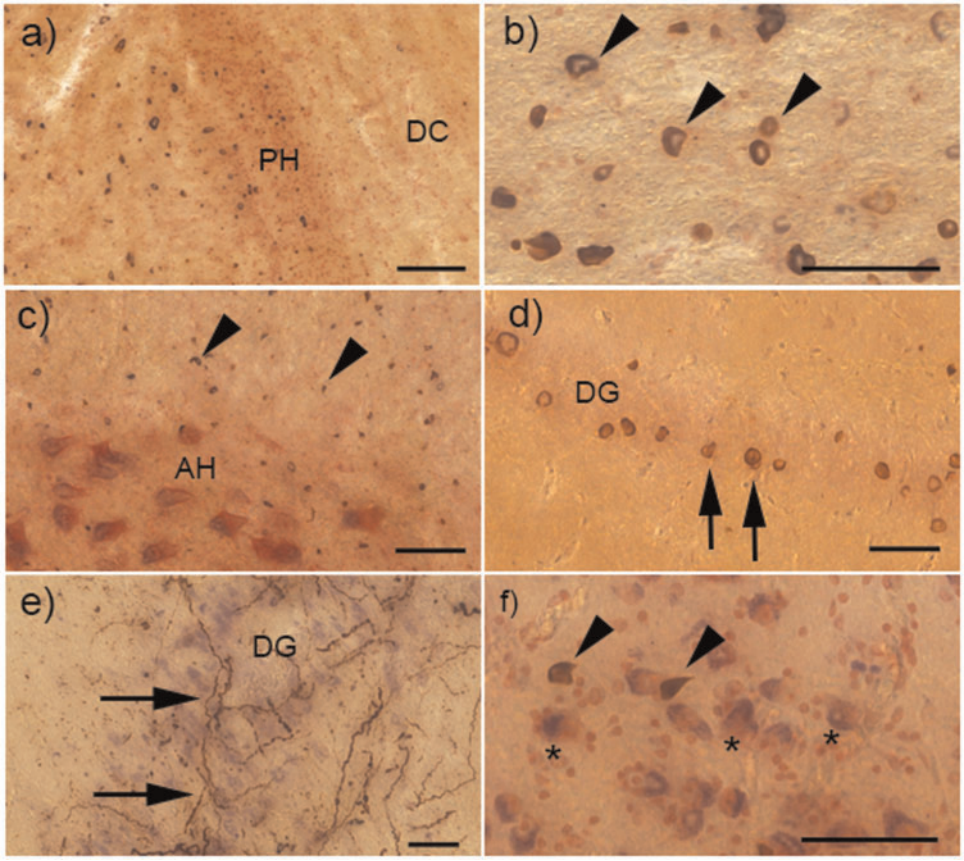

FIGURE 4. α-Synuclein (α-syn) pathology in the cervical spinal cord, hippocampus, and amygdala of cases with striatonigral degeneration (SND). **(A)** Shows multiple glial cytoplasmic inclusions (GCI) in the spinal cord white matter, though the dorsal column (DC) to the right of the posterior horn (PH) is only very mildly involved. **(B)** Multiple GCI (examples depicted by arrowheads) in the corticospinal tract. **(C)** Multiple GCI in the white matter surrounding the anterior horn (AH), and some GCI within the AH, but no neuronal inclusions (NI) can be seen. **(D)** NI within the dentate gyrus (DG) of the hippocampus (examples shown by arrows). **(E)** Severe neuritic inclusions (NRI) within the DG. **(F)** GCI (shown by arrowheads) among the neurons of the amygdala (examples depicted by asterisks). Scale bar in **(A)** = 100 μm; all other scale bars = 50 μm.

observed in the external plexiform layer as well as in the stratum radiatum et lacunosum, while NI were rarer and were first detected in the outer parts of the Ammon's horn (CA1, CA2) as well as in the subiculum. In contrast, the inner parts of the Ammon's horn (CA3, CA 4) and the dentate gyrus were less affected, and only became involved in the most severe cases (Figs. 2A, 4D). Occasionally, extensive NRI could be detected within the Ammon's horn (Fig. 4E). Hippocampal involvement was associated with the presence of α-syn pathology in the entorhinal cortex as well as in the basolateral subnucleus of the amygdala (Figs. 2A, 4F). Cortical involvement in phase 3 became more severe throughout but still did not involve the occipital cortex.

Phase 4: Involvement of the Occipital Neocortex

In SND cases with the longest disease duration (n = 13, mean duration of disease 134.4 months ± 33.8 months), α-syn inclusions disseminated to involve the visual cortex (Fig. 2A). In addition, these cases occasionally showed mild NI in the dentate nucleus of the cerebellum. The hypoglossal nucleus showed some GCI, but did not develop NI in these cases.

Comparing α-Syn Pathology in SND and OPCA

Following our analysis of phases of α-syn pathology in SND, we proceeded to compare patterns of α-syn pathology in cases with SND and OPCA. GCI pathology was more severe in SND as compared to OPCA in midbrain crus cerebri ($p = 0.03$). In contrast, GCI pathology was more severe in OPCA as compared to SND in the internal white matter of medulla ($p = 0.03$), inferior cerebellar peduncle ($p = 0.02$), and in the subcortical cerebellar white matter ($p = 0.04$). NI were more severe in OPCA (than SND) in hypoglossal nucleus as well as in the dentate nucleus of the cerebellum ($p = 0.002$). NI tended to be more severe in the dorsal motor nucleus of the vagus in the medulla in OPCA than SND, though the difference did not reach statistical significance ($p = 0.06$). Neuronal loss was more severe in SND as compared with OPCA in the striatum ($p < 0.01$) and the substantia nigra ($p = 0.04$), whereas neuronal loss was more severe in OPCA as compared

to SND in the inferior olive ($p = 0.002$) and the in medulla in general ($p = 0.03$). There was also a tendency towards higher neuronal loss in the red nucleus of OPCA as compared to SND, though that did just fail to reach statistical significance ($p = 0.05$).

While SND cases with the shortest disease duration showed most severe α-syn pathology in striatum, lentiform nucleus, and substantia nigra (phase 1, Fig. 2A), phase 1 cases with OPCA were characterized by the involvement of cerebellar subcortical white matter and cerebellar brainstem projections in medulla and pons (phase 1, Fig. 2A). However, these early foci were also already mildly involved in phase 1 or phase 2 cases of the other subtype of MSA pathology.

In both SND and OPCA, involvement of spinal cord and cortex was observed in phases 1 or 2 (Fig. 2A, B). In contrast, involvement of the amygdala and hippocampus was only observed in cases with a long disease duration in both SND (phase 3) and OPCA (phase 4). Similarly, the visual cortex showed only mild α-syn pathology and only became involved in cases with a long duration of disease (phase 4 in both SND and OPCA).

There was a marked similarity of regional distribution of pathology between SND and OPCA, especially in cases with longer disease duration (phase 3 and 4). As an example, cerebellar α-syn pathology in both SND and OPCA was most severe in the subcortical white matter, whereas granular layer and deep white matter were less affected, and molecular layer and Purkinje cell layer were free of pathology in both subtypes of MSA (Fig. 2A, B). In addition, CSC α-syn pathology in both SND and OPCA to a similar extent involved pyramidal and extra-pyramidal fiber tracts, but only mildly affected the dorsal column. Furthermore, cortical pathology in both SND and OPCA was most severe in the motor cortex, sensory cortex, and anterior cingulate gyrus, with milder involvement of other cortical regions (eg orbital gyrus, midfrontal cortex, SMT, angular cortex). In both SND and OPCA, involvement of the visual cortex was least severe and only found in cases with long disease duration (Fig. 2A, B). In the medulla, both MSA subtypes showed the most severe pathology in pyramidal fibers, internal white matter (olivo-cerebellar fibers), and inferior cerebellar peduncle, whereas the nuclei XII and X were least affected.

Clinico-Pathological Correlations

Nearly all patients with OPCA showed a clinical onset with a cerebellar syndrome (90%, Table), while a single case initially showed autonomic dysfunction (no. 38, Table). Most patients with SND (70.3%; $n = 26$) showed Parkinsonism as the first clinical symptom, whereas 10.8% ($n = 4$) first presented with autonomic dysfunction, and a single case with upper motor neuron involvement. In 6 cases (16.2%), clinical data on first clinical symptoms were equivocal. Development of cognitive impairment before death was reported in 7/38 cases with SND (18.4%), but in none of the OPCA cases. We observed no significant difference regarding age at onset or disease duration between the 2 pathological subtypes of MSA.

Disease duration correlated with severity of GCI pathology across many regions, including amygdala, hippocampus, orbital frontal cortex, middle frontal cortex, anterior cingulate gyrus, motor cortex, SMT, angular cortex, internal capsule in the striatum, corticospinal tract in the CSC, spinocerebellar tract in the CSC, spinothalamic fibers in the CSC, ($p < 0.01$ each), sensory cortex, lentiform nucleus, superior cerebellar peduncle in the pons ($p < 0.05$ each).

Disease duration also correlated with phases of α-syn pathology as proposed here ($p < 0.05$). It furthermore correlated with neuronal loss across many regions, including hippocampus, putamen, striatum, thalamus, substantia nigra, red nucleus, pons, cerebellum ($p < 0.01$ each) and medulla ($p < 0.05$). In contrast, disease duration correlated with severity of NI only in the dentate gyrus of the hippocampus ($p < 0.01$). Age of onset or age at death did not correlate with the severity of α-syn pathology or neuronal loss ($p > 0.05$ in each region).

Genetic Results

To identify genetic variants associated with disease, we sequenced genes known to be associated with MSA and α-syn pathology, including *COQ2*, *SNCA*, and *GBA* in 45 MSA cases (35 SND and 10 OPCA) and 10 normal controls for which genomic DNA was available. No pathogenic or likely pathogenic variants in *COQ2* or *SNCA* were identified in any of the cases. As the predominance of the MSA subtypes is population-based, we limited further genetic analysis to Caucasians (33 SND and 7 OPCA). A Gaucher disease *GBA* variant, NM_000157: c.1226A>G (p.Asn409Ser, legacy nomenclature Asn370Ser, rs76763715), was found as heterozygous in 1 of 7 cases with OPCA subtype (minor allele frequency [MAF] 7.1%), the significance of which is unclear due to the small sample size. On the other hand, a different heterozygous missense variant in *GBA*, c.1223C>T (p.Thr408Met, legacy nomenclature Thr369Met, rs75548401) was identified in 4 of 33 SND cases, corresponding to an MAF of 6.1%, which is about 6 times higher compared to the European population frequency in the Exome Aggregation Consortium database (EXAC, http://exac.broadinstitute.org; Last accessed August 20, 2018) of 1% for p.Thr408Met. The genotypes were all confirmed by TaqMan genotyping. To further evaluate whether the *GBA* p.Thr408Met variant is associated with an increased risk of MSA, 312 additional neuropathologically confirmed Caucasian cases (251 brains with nonMSA neurodegenerative diseases; 7 additional MSA cases [3 SND and 4 OPCA subtypes]; and 54 brains with no neuropathological evidence of disease) were either genotyped for the rs75548401 variant by TaqMan assay or by sequencing (Supplementary Data Tables S1, S2). In total, 5 of 36 Caucasian SND cases carried heterozygous p.Thr408Met (MAF 6.94%), whereas only 3 of 204 brains with various nonMSA neuropathologies (1 amyotrophic lateral sclerosis [ALS] and 2 FTLD-TDP cases) carried the variant (MAF 0.7%, $p = 0.0019$). None of the normal brains ($n = 54$) or MSA OPCA subtype cases ($n = 11$) were found to have the p.Thr408Met variant. This result demonstrates that the frequency of *GBA* variant p.Thr408Met in MSA SND subtype cases is significantly higher compared with the other cohorts (Supplementary Data Table S2), suggesting that the *GBA* variant p.Thr408Met is

associated with MSA, and in particular, the SND subtype. The result in the present study further supports the previously published data that the *GBA* variant p.Thr408Met may increase the risk for MSA (33–35).

DISCUSSION

GCI and Neuronal Loss in SND and OPCA

In line with previous reports by our group and others (2, 12, 13, 25, 36–45), we found GCI to be the predominant α-syn pathology in both SND and OPCA, while NI and NRI were less prevalent. Remarkably, neuronal loss frequently occurred in groups of neurons that did not (or only to a very mild extent) show NI. As an example, neuronal loss in the SN was observed in early phases of SND without presence of NI in the dopaminergic pigmented neurons themselves. However, these cases showed severe GCI pathology in the internal capsule (Fig. 1B) and the crus cerebri, which both contain neuronal connections of SN neurons. This suggests that oligodendroglial α-syn aggregation and the associated neuronal dysfunction and loss could be located in anatomically distant regions, a notion that is also supported by neuroimaging studies (46, 47). Moreover, regional severity of α-syn pathology and neuronal loss only rarely correlated in this study, in contrast to observations on other synucleinopathies like PD and TDP-43 proteinopathies including ALS, where neuronal loss frequently correlates with severity of neuronal aggregation of α-syn or TDP-43 (22, 28, 48, 49). Consequently, neuronal vulnerability in MSA could be determined by the involvement of anatomically distant white matter tracts containing connections of these vulnerable neurons.

The mechanism by which α-syn accumulation causes neuronal dysfunction and death in MSA is unclear. There is increasing evidence that oligodendrocytes provide essential metabolic support to neurons by transferring glycolytic intermediates through the monocarboxylic transporter MCT1 (50, 51). Furthermore, oligodendrocytes are responsible for maintaining brain lipid homeostasis in the form of the specialized myelin membrane. Myelin instability, possibly mediated by abnormalities of ABCA8 lipid transporter expression, was suggested to precede α-syn pathology in MSA (52, 53). Consequently, the axonal support provided by oligodendrocytes through myelination, trophic factors, and energy metabolites (54) could be impaired in MSA, thereby leading to neuronal loss.

Phases of Pathology in SND

We proceeded to analyze patterns of pathology in MSA cases with an increasing disease duration and overall burden of α-syn aggregates. Our aim was not to establish a new grading system of MSA, as previous efforts exist including a detailed analysis of basal ganglia involvement (12, 36) and as the numbers of cases in the early phases described here were rather low, but to determine early foci of MSA pathology. To establish a novel staging of MSA, we believe our study has to be followed by a multi-center approach including higher numbers of autopsy cases.

In line with previous observations, we found the most severe α-syn pathology in SND with a short duration of disease (phase 1, mean duration of disease 48 months, Fig. 2A) to be located in the striatum as well as the SN (12, 40, 55–57).

In the midbrain, earliest GCI and NRI prominently involved the crus cerebri, which contains the striatonigral "comb" fibers (58), whose involvement could be linked to neuronal loss in the SN which is a key feature of MSA noted by earlier studies (12, 36, 59). Similarly, severe GCI and NRI in the internal capsule of phase 1 cases could contribute to neuronal loss in the putamen and SN. Though the dorsolateral putamen was most severely involved, a detailed analysis of basal ganglia pathology would profit from analysis of serial hemispheral sections of the basal ganglia, which were not available for this study.

In accordance with previous observations (12, 36, 56), we observed widespread spinal cord pathology in SND from phase 2 onwards. This was observed to affect white matter tracts including the corticospinal, spino-thalamic, spino-cerebellar, and spino-olivary tract but was also detected in the spinal cord grey matter. Spinal cord oligodendroglial pathology is usually minor in most neurodegenerative diseases, but was also observed to be extensive in ALS, another nonprion neurodegenerative disease, suggesting that white matter oligodendroglia and nonmyelinating grey matter oligodendroglia could play an important role in some protein propagation diseases (20, 60). Spinal cord α-syn pathology included loss of intermediolateral neurons, which has classically been considered a substrate of sympathetic nervous system failure in MSA (56, 61–63). However, only 3 cases with spinal cord sections below the CSC were available here. Consequently, further detailed studies of full-length spinal cords will be necessary to elucidate the severity of IML involvement in MSA.

From phase 1 onward, α-syn inclusions were detectable in the neocortex, initially mainly involving the motor and middle frontal cortex (Brodmann 4, 6) before spreading to other prefrontal, temporal, and parietal cortical regions. Importantly, both the motor cortex and the anterior cingulate gyrus project to the striatum (64, 65), suggesting that GCI pathology in the white matter of these regions could be linked to striatal neuronal dysfunction and loss. Although cortical involvement in MSA is generally considered to be rare (66), some studies showed neuronal loss in the motor and supplementary motor cortex (67), and suggested a relation to striato-nigral involvement (68).

We observed involvement of the hippocampus, basolateral subnucleus of the amygdala and entorhinal cortex to occur only in phase 3 SND cases (Fig. 4D–F). This is in line with previous reports which suggested a relative preservation of limbic structures in MSA (66), and observed hippocampal atrophy only in some cases with a long progression of disease using voxel-based morphometry (69). These cases were also characterized by severe and widespread α-syn pathology in the spinal cord, which included the posterior columns of the spinal cord. Finally, and in line with previous reports, our study suggests that involvement of the visual cortex is rare in MSA and only found in cases with a long disease duration (66).

Comparing SND and OPCA Cases

Different Early Foci of α-Syn Pathology in SND and OPCA

Following analysis of phases of α-syn pathology in SND, we proceeded to compare patterns of α-syn pathology in SND and OPCA. Generally, SND and OPCA cases presented with the same basic morphological types of α-syn aggregates (eg predominant GCI, less severe NRI and NI). In accordance with previous findings (12, 36, 66), we observed the anatomical distribution patterns of α-syn pathology in SND and OPCA cases with a short duration of disease (phases 1 and 2, mean duration of disease 51.4 months ± 12.8 months, Fig. 2A, B) to be clearly distinct, indicating different early foci of pathology.

Increasing Overlap of α-Syn Pathology With Progression of Disease

While we observed different early foci of α-syn pathology in SND and OPCA, patterns of pathology increasingly overlapped in cases with longer disease duration (phases 3 and 4, mean duration of disease 113 months ± 35.2 months), which has also been noted by several previous studies (6, 12, 36, 45, 57, 66, 67). As an example, phase 3 and 4 SND cases showed moderate to severe α-syn inclusions in the cerebellum and cerebellar white matter connections in the brainstem, whereas phase 3 and 4 OPCA cases showed considerable pathology in basal ganglia and SN. In addition, spreading patterns of SND and OPCA showed similar directions with increasing duration of disease: In both SND and OPCA, the thalamus became involved in phase 2, and amygdala and hippocampus became involved in phase 3. Finally, involvement of the visual cortex was only found in phase 4 cases of both SND and OPCA.

Similar Regional Patterns of α-Syn Pathology in SND and OPCA

We not only observed an increasing overlap of α-syn pathology with increasing duration of disease, but also noted anatomical distribution patterns within the regions analyzed here that were strikingly similar between SND and OPCA. As an example, cases with SND showed cerebellar pathology that was highly similar to what we and others observed to be characteristic of OPCA cases (12, 25, 41, 59, 70), with most severe involvement of subcortical white matter, milder pathology in the granular layer and deep white matter, and sparing of molecular layer and Purkinje cell layer (Fig. 3A–C). Thus, even though cerebellar involvement in SND is less severe and occurs later than in OPCA, it affects the same anatomical structures. Likewise, both types of MSA showed similar anatomical distribution patterns of α-syn pathology in cortical areas, with subcortical white matter most severely affected, and cortical grey matter only involved to a lesser extent. In addition, both SND and OPCA showed an early involvement of the motor cortex and a very late affection of occipital areas (Fig. 2A, B). Finally, both OPCA and SND showed a similar pattern of involvement of the spinal cord, with pyramidal and extrapyramidal fiber tracts being most severely affected, whereas the dorsal column showed only mild pathology in both subtypes of MSA (Fig. 4A–C).

Taken together, these findings indicate that SND and OPCA show distinct early foci of α-syn aggregations, but increasingly converge with longer disease duration to show overlapping patterns of α-syn pathology. This supports the notion of both MSA subtypes as different variants of a single disease rather than separate entities (71).

Genetic Risk for MSA

Genetic variants in *GBA*, mutations of which cause Gaucher disease, an autosomal recessive lysosomal storage disease, have previously been associated with an approximate 5-fold increased risk for PD and other synucleinopathies, such as DLB, in heterozygous carriers of genetic variants in *GBA* (34). In addition, PD patients with *GBA* mutations may have earlier onset of symptoms and an increased risk for cognitive changes (72). The mechanism for the increased risk of disease may involve functional loss of glucocerebrosidase, which compromises lysosomal protein degradation, causes accumulation of α-syn, and results in neurotoxicity through aggregation dependent mechanisms (73). While initial studies have focused on *GBA* variants that are pathogenic for Gaucher disease, 2 *GBA* variants, p.Thr408Met and p.Glu365Lys, which are not considered to be pathogenic for Gaucher disease, were found to be significantly enriched in PD patients compared with controls (33). Furthermore, in their study, Benitez et al found that the p.Thr408Met variant in *GBA* appeared to be the primary driver of the association with PD (33). This is interesting because in this study we observed the p.Thr408Met variant in 13.9% (5 of 36) of Caucasian cases of SND subtype of MSA with a MAF of 6.94%. In our experience of sequencing *GBA* in autopsy cases (n = 204) with other neurodegenerative disease pathologies including Alzheimer disease, ALS, frontotemporal lobar degeneration, and Lewy body disorders (Supplementary Data Table S1), only 3 cases with the p.Thr408Met variant were identified, corresponding to an odds ratio of 10.07 (95% confidence interval 2.35–43.14) with a p value of 0.0019 compared to SND. While the number of cases in our study is small, a similar result showing increased frequency of *GBA* variants in MSA, including p.Thr408Met, has been recently published (35). Further study and replication of the finding are needed to confirm the association and to evaluate the genotype-phenotype correlations of p.Thr408Met versus other *GBA* variants and pathogenic mutations and whether there is any difference in genetic risk association of *GBA* variants between SND and OPCA subtypes of MSA.

Transmission of α-Syn Pathology in MSA?

Here, we demonstrate a stereotypical pattern of sequential regional involvement in cases with SND that correlated with duration of disease. A similar spreading pattern has previously been described for PD and DLB (22, 48, 74–81). However, evidence that this concept could also be valid in MSA is just beginning to emerge (82–84).

While we observed a stereotypical spreading pattern that correlated with progression of disease, we were not able to identify a single focal onset of disease pathology. Rather, we identified several different white matter fiber tracts as early foci of pathology in SND. Our study was further limited by the comparative lack of early stage cases (out of 47 cases with MSA, only 5 cases with a phase 1 were available). Consequently, further studies of early-stage cases with MSA will be necessary to validate our findings and to further delineate the onset of MSA pathology.

REFERENCES

1. Krismer F, Wenning GK. Multiple system atrophy: Insights into a rare and debilitating movement disorder. Nat Rev Neurol 2017;13:232–43
2. Trojanowski JQ, Revesz T. Neuropathology Working Group on MSA. Proposed neuropathological criteria for the post mortem diagnosis of multiple system atrophy. Neuropathol Appl Neurobiol 2007;33:615–20
3. Tison F, Yekhlef F, Chrysostome V, et al. Parkinsonism in multiple system atrophy: Natural history, severity (UPDRS-III), and disability assessment compared with Parkinson's disease. Mov Disord 2002;17:701–9
4. Lin DJ, Hermann KL, Schmahmann JD. Multiple system atrophy of the cerebellar type: Clinical state of the art. Mov Disord 2014;29:294–304
5. Watanabe H, Saito Y, Terao S, et al. Progression and prognosis in multiple system atrophy: An analysis of 230 Japanese patients. Brain 2002; 125:1070–83
6. Ahmed Z, Asi YT, Sailer A, et al. The neuropathology, pathophysiology and genetics of multiple system atrophy. Neuropathol Appl Neurobiol 2012;38:4–24
7. Figueroa JJ, Singer W, Parsaik A, et al. Multiple system atrophy: Prognostic indicators of survival. Mov Disord 2014;29:1151–7
8. Scholz SW, Houlden H, Schulte C, et al. SNCA variants are associated with increased risk for multiple system atrophy. Ann Neurol 2009;65: 610–4
9. Mitsui J, Tsuji S. Mutant COQ2 in multiple-system atrophy. N Engl J Med 2014;371:82–3
10. Sailer A, Scholz SW, Nalls MA, et al. A genome-wide association study in multiple system atrophy. Neurology 2016;87:1591–8
11. Sharma M, Wenning G, Kruger R. Mutant COQ2 in multiple-system atrophy. N Engl J Med 2014;371:80–1
12. Wenning GK, Seppi K, Tison F, et al. A novel grading scale for striatonigral degeneration (multiple system atrophy). J Neural Transm 2002; 109:307–20
13. Tu PH, Galvin JE, Baba M, et al. Glial cytoplasmic inclusions in white matter oligodendrocytes of multiple system atrophy brains contain insoluble alpha-synuclein. Ann Neurol 1998;44:415–22
14. Abeliovich A, Schmitz Y, Farinas I, et al. Mice lacking alpha-synuclein display functional deficits in the nigrostriatal dopamine system. Neuron 2000;25:239–52
15. Jo E, McLaurin J, Yip CM, et al. alpha-Synuclein membrane interactions and lipid specificity. J Biol Chem 2000;275:34328–34
16. Logan T, Bendor J, Toupin C, et al. alpha-Synuclein promotes dilation of the exocytotic fusion pore. Nat Neurosci 2017;20:681–9
17. Spillantini MG, Crowther RA, Jakes R, et al. alpha-Synuclein in filamentous inclusions of Lewy bodies from Parkinson's disease and dementia with lewy bodies. Proc Natl Acad Sci U S A 1998;95:6469–73
18. Jucker M, Walker LC. Self-propagation of pathogenic protein aggregates in neurodegenerative diseases. Nature 2013;501:45–51
19. Guo JL, Lee VM. Cell-to-cell transmission of pathogenic proteins in neurodegenerative diseases. Nat Med 2014;20:130–8
20. Brettschneider J, Del Tredici K, Lee VM, et al. Spreading of pathology in neurodegenerative diseases: A focus on human studies. Nat Rev Neurosci 2015;16:109–20
21. Feldengut S, Del Tredici K, Braak H. Paraffin sections of 70–100 μm: A novel technique and its benefits for studying the nervous system. J Neurosci Methods 2013;215:241–4
22. Braak H, Del Tredici K, Rub U, et al. Staging of brain pathology related to sporadic Parkinson's disease. Neurobiol Aging 2003;24:197–211
23. Gilman S, Low PA, Quinn N, et al. Consensus statement on the diagnosis of multiple system atrophy. J Neurol Sci 1999;163:94–8
24. Gilman S, Wenning GK, Low PA, et al. Second consensus statement on the diagnosis of multiple system atrophy. Neurology 2008;71:670–6
25. Brettschneider J, Irwin DJ, Boluda S, et al. Progression of alpha-synuclein pathology in multiple system atrophy of the cerebellar type. Neuropathol Appl Neurobiol 2017;43:315–29
26. Toledo JB, Van Deerlin VM, Lee EB, et al. A platform for discovery: The University of Pennsylvania Integrated Neurodegenerative Disease Biobank. Alzheimers Dement 2014;10:477–84
27. Xie SX, Baek Y, Grossman M, et al. Building an integrated neurodegenerative disease database at an academic health center. Alzheimers Dement 2011;7:e84–93
28. Brettschneider J, Del Tredici K, Toledo JB, et al. Stages of pTDP-43 pathology in amyotrophic lateral sclerosis. Ann Neurol 2013;74:20–38
29. Geser F, Brandmeir NJ, Kwong LK, et al. Evidence of multisystem disorder in whole-brain map of pathological TDP-43 in amyotrophic lateral sclerosis. Arch Neurol 2008;65:636–41
30. Duda JE, Giasson BI, Mabon ME, et al. Novel antibodies to synuclein show abundant striatal pathology in Lewy body diseases. Ann Neurol 2002;52:205–10
31. Neumann M, Kwong LK, Lee EB, et al. Phosphorylation of S409/410 of TDP-43 is a consistent feature in all sporadic and familial forms of TDP-43 proteinopathies. Acta Neuropathol 2009;117:137–49
32. Lee EB, Leng LZ, Zhang B, et al. Targeting amyloid-beta peptide (Abeta) oligomers by passive immunization with a conformation-selective monoclonal antibody improves learning and memory in Abeta precursor protein (APP) transgenic mice. J Biol Chem 2006;281:4292–9
33. Benitez BA, Davis AA, Jin SC, et al. Resequencing analysis of five Mendelian genes and the top genes from genome-wide association studies in Parkinson's Disease. Mol Neurodegener 2016;11:29
34. Siebert M, Sidransky E, Westbroek W. Glucocerebrosidase is shaking up the synucleinopathies. Brain 2014;137:1304–22
35. Sklerov M, Kang UJ, Liong C, et al. Frequency of GBA variants in autopsy-proven multiple system atrophy. Mov Disord Clin Pract 2017;4: 574–81
36. Jellinger KA, Seppi K, Wenning GK. Grading of neuropathology in multiple system atrophy: Proposal for a novel scale. Mov Disord 2005; 20(Suppl. 12):S29–36
37. Arnold SE, Toledo JB, Appleby DH, et al. Comparative survey of the topographical distribution of signature molecular lesions in major neurodegenerative diseases. J Comp Neurol 2013;521:4339–55
38. Mochizuki Y, Mizutani T, Warabi Y, et al. The somatosensory cortex in multiple system atrophy. J Neurol Sci 2008;271:174–9
39. Sakamoto M, Uchihara T, Nakamura A, et al. Progressive accumulation of ubiquitin and disappearance of alpha-synuclein epitope in multiple system atrophy-associated glial cytoplasmic inclusions: Triple fluorescence study combined with Gallyas-Braak method. Acta Neuropathol 2005;110:417–25
40. Armstrong RA, Lantos PL, Cairns NJ. Spatial patterns of alpha-synuclein positive glial cytoplasmic inclusions in multiple system atrophy. Mov Disord 2004;19:109–12
41. Nishie M, Mori F, Fujiwara H, et al. Accumulation of phosphorylated alpha-synuclein in the brain and peripheral ganglia of patients with multiple system atrophy. Acta Neuropathol 2004;107:292–8
42. Gai WP, Pountney DL, Power JH, et al. alpha-Synuclein fibrils constitute the central core of oligodendroglial inclusion filaments in multiple system atrophy. Exp Neurol 2003;181:68–78
43. Dickson DW, Liu W, Hardy J, et al. Widespread alterations of alpha-synuclein in multiple system atrophy. Am J Pathol 1999;155:1241–51
44. Spillantini MG, Crowther RA, Jakes R, et al. Filamentous alpha-synuclein inclusions link multiple system atrophy with Parkinson's disease and dementia with Lewy bodies. Neurosci Lett 1998; 251:205–8
45. Ozawa T, Paviour D, Quinn NP, et al. The spectrum of pathological involvement of the striatonigral and olivopontocerebellar systems in multiple system atrophy: Clinicopathological correlations. Brain 2004;127: 2657–71
46. Lu CF, Wang PS, Lao YL, et al. Medullo-ponto-cerebellar white matter degeneration altered brain network organization and cortical morphology in multiple system atrophy. Brain Struct Funct 2014;219:947–58
47. Lu CF, Soong BW, Wu HM, et al. Disrupted cerebellar connectivity reduces whole-brain network efficiency in multiple system atrophy. Mov Disord 2013;28:362–9

48. Del Tredici K, Braak H. Spinal cord lesions in sporadic Parkinson's disease. Acta Neuropathol 2012;124:643–64
49. Brettschneider J, Del Tredici K, Irwin DJ, et al. Sequential distribution of pTDP-43 pathology in behavioral variant frontotemporal dementia (bvFTD). Acta Neuropathol 2014;127:423–39
50. Horner PJ, Thallmair M, Gage FH. Defining the NG2-expressing cell of the adult CNS. J Neurocytol 2002;31:469–80
51. Lee Y, Morrison BM, Li Y, et al. Oligodendroglia metabolically support axons and contribute to neurodegeneration. Nature 2012;487:443–8
52. Bleasel JM, Wong JH, Halliday GM, et al. Lipid dysfunction and pathogenesis of multiple system atrophy. Acta Neuropathol Commun 2014;2:15
53. Bleasel JM, Hsiao JH, Halliday GM, et al. Increased expression of ABCA8 in multiple system atrophy brain is associated with changes in pathogenic proteins. J Parkinsons Dis 2013;3:331–9
54. Nave KA, Trapp BD. Axon-glial signaling and the glial support of axon function. Annu Rev Neurosci 2008;31:535–61
55. Wenning GK, Ben-Shlomo Y, Magalhaes M, et al. Clinicopathological study of 35 cases of multiple system atrophy. J Neurol Neurosurg Psychiatry 1995;58:160–6
56. Wenning GK, Tison F, Ben Shlomo Y, et al. Multiple system atrophy: A review of 203 pathologically proven cases. Mov Disord 1997;12:133–47
57. Armstrong RA, Cairns NJ, Lantos PL. Multiple system atrophy (MSA): Topographic distribution of the alpha-synuclein-associated pathological changes. Parkinsonism Relat Disord 2006;12:356–62
58. Fox CA, Rafols JA. The striatal efferents in the globus pallidus and in the substantia nigra. Res Publ Assoc Res Nerv Ment Dis 1976;55:37–55
59. Wenning GK, Tison F, Elliott L, et al. Olivopontocerebellar pathology in multiple system atrophy. Mov Disord 1996;11:157–62
60. Brettschneider J, Arai K, Del Tredici K, et al. TDP-43 pathology and neuronal loss in amyotrophic lateral sclerosis spinal cord. Acta Neuropathol 2014;128:423–37
61. Oppenheimer DR. Lateral horn cells in progressive autonomic failure. J Neurol Sci 1980;46:393–404
62. Cersosimo MG, Benarroch EE. Central control of autonomic function and involvement in neurodegenerative disorders. Handb Clin Neurol 2013;117:45–57
63. Ozawa T. Morphological substrate of autonomic failure and neurohormonal dysfunction in multiple system atrophy: Impact on determining phenotype spectrum. Acta Neuropathol 2007;114:201–11
64. Ferry AT, Ongur D, An X, et al. Prefrontal cortical projections to the striatum in macaque monkeys: Evidence for an organization related to prefrontal networks. J Comp Neurol 2000;425:447–70
65. McFarland NR, Haber SN. Convergent inputs from thalamic motor nuclei and frontal cortical areas to the dorsal striatum in the primate. J Neurosci 2000;20:3798–813
66. Ramirez EP, Vonsattel JP. Neuropathologic changes of multiple system atrophy and diffuse Lewy body disease. Semin Neurol 2014;34:210–6
67. Tsuchiya K, Ozawa E, Haga C, et al. Constant involvement of the Betz cells and pyramidal tract in multiple system atrophy: A clinicopathological study of seven autopsy cases. Acta Neuropathol 2000;99:628–36
68. Su M, Yoshida Y, Hirata Y, et al. Primary involvement of the motor area in association with the nigrostriatal pathway in multiple system atrophy: Neuropathological and morphometric evaluations. Acta Neuropathol 2001;101:57–64
69. Brenneis C, Egger K, Scherfler C, et al. Progression of brain atrophy in multiple system atrophy. A longitudinal VBM study. J Neurol 2007;254:191–6
70. Mori F, Piao YS, Hayashi S, et al. Alpha-synuclein accumulates in Purkinje cells in Lewy body disease but not in multiple system atrophy. J Neuropathol Exp Neurol 2003;62:812–9
71. Wenning GK, Geser F, Krismer F, et al. The natural history of multiple system atrophy: A prospective European cohort study. Lancet Neurol 2013;12:264–74
72. Malec-Litwinowicz M, Rudzinska M, Szubiga M, et al. Cognitive impairment in carriers of glucocerebrosidase gene mutation in Parkinson disease patients. Neurol Neurochir Pol 2014;48:258–61
73. Mazzulli JR, Xu YH, Sun Y, et al. Gaucher disease glucocerebrosidase and alpha-synuclein form a bidirectional pathogenic loop in synucleinopathies. Cell 2011;146:37–52
74. Hansen C, Angot E, Bergstrom AL, et al. alpha-Synuclein propagates from mouse brain to grafted dopaminergic neurons and seeds aggregation in cultured human cells. J Clin Invest 2011;121:715–25
75. Kordower JH, Dodiya HB, Kordower AM, et al. Transfer of host-derived alpha synuclein to grafted dopaminergic neurons in rat. Neurobiol Dis 2011;43:552–7
76. Volpicelli-Daley LA, Luk KC, Patel TP, et al. Exogenous alpha-synuclein fibrils induce Lewy body pathology leading to synaptic dysfunction and neuron death. Neuron 2011;72:57–71
77. Mougenot AL, Nicot S, Bencsik A, et al. Prion-like acceleration of a synucleinopathy in a transgenic mouse model. Neurobiol Aging 2012;33:2225–8
78. Masuda-Suzukake M, Nonaka T, Hosokawa M, et al. Prion-like spreading of pathological alpha-synuclein in brain. Brain 2013;136:1128–38
79. Luk KC, Kehm V, Carroll J, et al. Pathological alpha-synuclein transmission initiates Parkinson-like neurodegeneration in nontransgenic mice. Science 2012;338:949–53
80. Luk KC, Kehm VM, Zhang B, et al. Intracerebral inoculation of pathological alpha-synuclein initiates a rapidly progressive neurodegenerative alpha-synucleinopathy in mice. J Exp Med 2012;209:975–86
81. Frost B, Diamond MI. Prion-like mechanisms in neurodegenerative diseases. Nat Rev Neurosci 2010;11:155–9
82. Reyes JF, Rey NL, Bousset L, et al. Alpha-synuclein transfers from neurons to oligodendrocytes. Glia 2014;62:387–98
83. Watts JC, Giles K, Oehler A, et al. Transmission of multiple system atrophy prions to transgenic mice. Proc Natl Acad Sci U S A 2013;110:19555–60
84. Peng C, Gathagan RJ, Covell DJ, et al. Cellular milieu imparts distinct pathological α-synuclein strains in α-synucleinopathies. Nature 2018;557:558–63